Hindawi Publishing Corporation
EURASIP Journal on Wireless Communications and Networking
Volume 2010, Article ID 465632, 13 pages
doi:10.1155/2010/465632

Research Article

Particle Swarm Optimization for Adaptive Resource Allocation in Communication Networks

Shahin Gheitanchi, Falah Ali, and Elias Stipidis

School of Engineering & Design, University of Sussex, Falmer, Brighton BN1 9QT, UK

Correspondence should be addressed to Falah Ali, f.h.ali@sussex.ac.uk

Received 13 January 2010; Revised 25 May 2010; Accepted 6 July 2010

Academic Editor: Hyunggon Park

A generalized model of particle swarm optimization (PSO) technique is proposed as a low complexity method for adaptive centralized and distributed resource allocation in communication networks. The proposed model is applied to adaptive multicarrier cooperative communications (MCCC) technique which utilizes the subcarriers in deep fade using a relay node in order to improve the bandwidth efficiency. Centralized PSO, based on virtual particles (VPs), is introduced for single layer and cross-layer subcarrier allocation to improve the bit error rate performance in multipath frequency selective fading channels. In the single layer strategy, the subcarriers are allocated based on the channel gains. In the cross-layer strategy, the subcarriers are allocated based on a joint measure of channel gains and distance provided by the physical layer and network layer to mitigate the effect of path loss. The concept of training particles in distributed PSO is proposed and then is applied for relay node selection. The computational complexity and traffic of the proposed techniques are investigated, and it is shown that using PSO for subcarrier allocation has a lower complexity than the techniques in the literature. Significant reduction in the traffic overhead of PSO is demonstrated when using trained particles in distributed optimizations.

1. Introduction

Particle swarm optimization (PSO) [1] is an optimization technique inspired from the interaction between swarm members that requires no supervision or prior knowledge and is based on primitive instincts. PSO technique has been applied to different layers of the open system interconnection (OSI) multilayer reference model which is designed for standard separation of network functionalities in communication systems [2]. In the OSI reference model, each layer exchanges data with adjacent layers in a node whilst allowing communication between peer layers with other nodes using a stack of protocols. To increase the efficiency and performance of each layer, the PSO technique has been utilized for single layer optimizations [3–9]. Recently, PSO has been applied for physical layer optimizations [3, 4]. For example in [4], PSO with virtual particles (VPs) is applied for resource allocation in orthogonal frequency division multiple access (OFDMA) where the subcarriers with the higher channel gains are adaptively allocated to users. In the literature, PSO has mostly been used for clustering of nodes in ad hoc networks aiming to minimize energy consumption [6–8]. In [6] the authors have applied PSO to cluster head selection, and in [7] it has been used for distance-based clustering of wireless sensor networks. Furthermore, in [8] PSO is employed to optimize the cost and coverage of clustering in mobile ad hoc networks. Many other applications for PSO in communications such as IP multicasting and channel assignment only have been mentioned in [9]. Using PSO in ad hoc network optimization increases flexibility, adaptation and robustness. While this optimization method is simple, it introduces enormous traffic and computation overhead to the network.

In this paper, a generalized PSO model for adaptive resource allocation in communication networks is proposed which can be applied for single layer and cross-layer optimizations. It consists of PSO with VPs [4] for centralized scenarios and trained PSO (TPSO) [5] for distributed scenarios. The proposed model is applied to the adaptive multicarrier cooperative communication (MCCC)

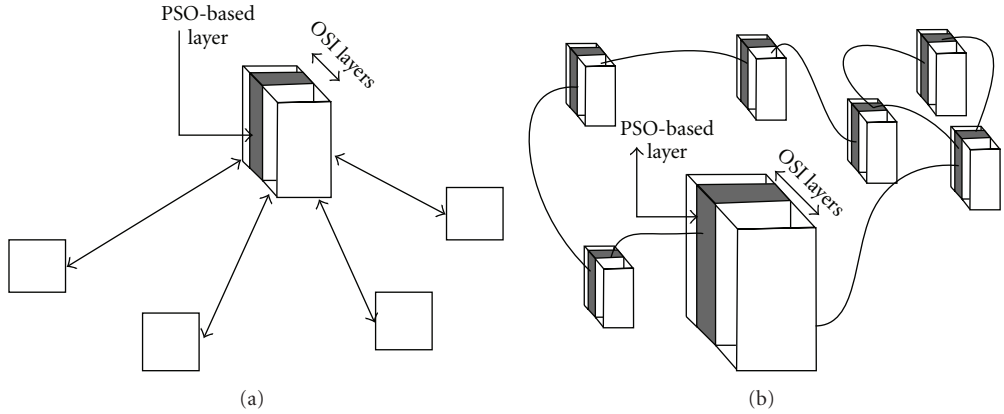

Figure 1: (a) Network model for centralized PSO in a single node. (b) Network model for distributed PSO in an ad hoc network using different nodes in the system.

technique [10] that utilizes a relay node to use the subcarriers with low channel gain to improve bandwidth efficiency. In a single layer strategy, the centralized PSO is used in the physical layer to reduce the computational complexity of subcarrier allocation. In a cross-layer strategy, centralized PSO is applied for subcarrier allocation based on a joint measure of node distances and channel gains to mitigate the effect of path loss. Distributed TPSO is employed for adaptive relay node selection in MCCC to reduce the traffic overhead.

In the rest of this paper, in Section 2, scope of PSO in communication networks is introduced. Next, in Section 3, a generalized PSO model for adaptive communication systems is proposed. In Section 4, the adaptive MCCC system model is explained. In Section 5, centralized and distributed PSO-aided resource allocation techniques in adaptive MCCC are introduced. In Section 6, the computational complexity and traffic overhead of the proposed techniques are investigated. In Section 7, the bit error rate performance is investigated by simulation. Finally, the paper is concluded.

2. Scope of PSO in Communication Networks

Based on the execution location of PSO algorithm, the optimization process is divided to centralized and distributed. In centralized PSO, the optimization is performed in a single node of a network. However, depending on the objective and the method of optimization, PSO process can run in more than one node and can be distributed over multiple nodes within the network. Figure 1(a) shows a centralized PSO for single node optimization, and Figure 1(b) shows distributed PSO over multinodes in an ad hoc network.

In many optimization processes the data is collected from more than one layer to achieve the objective of the process [11]. These processes are referred to as cross-layer optimizations. The centralized PSO for cross-layer optimization in a single node is divided to three categories as shown in Figure 2 for seven layer OSI network model.

(1) The optimization is performed using one PSO process in a single layer, and the needed data for optimization is provided by one or many other layers.

(2) The optimization is performed in multi-PSO processes in different layers. In this case, all the involved layers of the node interact with each other to share the data and the processing load.

(3) The optimization is performed in one PSO process in an extralayer dedicated to the optimization process. This layer is responsible for the collection and processing of the data from one or more layers of a node.

Furthermore, the cross-layer optimization process can also be centralized in one node or be distributed over multiple nodes.

3. Generalized PSO Model

In this section, a generalized model of PSO is proposed which will be utilized for adaptive resource allocation in MCCC technique. In PSO, individual members of swarm are called particles. Each particle keeps track of its coordinates in the problem space which are associated with the best solution (fitness) it has achieved so far. The best solution found by a particle is called the personal best (PB). Additionally each particle has knowledge of the best solution found by nearby particles, called the global best (GB). Particles act individually under the same principle: accelerate toward the PB and GB locations while constantly checking the fitness value of current location. In the proposed generalized PSO model, P particles with unique particle IDs (PIDs) are randomly distributed over solution space. The solution space, S, is the set of all possible solutions for the optimization problem. Depending on the problem, the solution space can have M number of dimensions where the mth dimension, S^m, contains N elements, s_n^m. Each particle is capable of measuring the suitability of solutions by using the fitness function $f(S^1, S^2, \ldots, S^M)$. All particles use a unique fitness

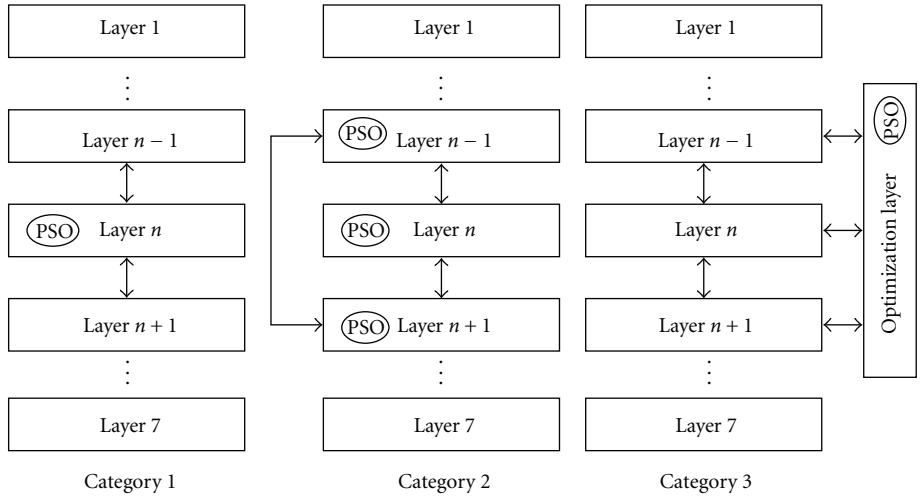

Figure 2: Centralized PSO for cross-layer optimization scenarios in a single node.

function to be able to compare the suitability of the solutions. PSO is flexible in that the optimization objective can be changed by modifying the fitness function. It should be noted that modification to the fitness function can affect the overall computational complexity. A mathematically complex function for calculating the fitness value has a greater computational requirement in the execution environment than a simple function. Therefore, for efficiency purposes utilization of a low complexity fitness function is recommended. The objective of the optimization is to find elements in solution spaces that maximize the fitness, $\hat{S} = (\hat{s}^1, \hat{s}^1, \ldots, \hat{s}^M)$, described as

$$\hat{S} = \text{Argmax}\, f\left(S^1, S^2, \ldots, S^M\right). \tag{1}$$

Assuming synchronized timing and identical speed among the particles, the optimization is performed during Γ iterations. At each iteration, the particles compare the PB and the GB to choose a direction independently based on the distance differences from current location to the GB and to the PB locations. To have a more practical model in resource limited communication networks, the particle decision making mechanism of the proposed model is simplified compared to the original PSO described in [1]. The physical distance between two locations, (s_1^1, s_2^1) and (s_1^2, s_2^2) for $M = 2$ is given by

$$d = \sqrt{\left(s_1^2 - s_1^1\right)^2 + \left(s_2^2 - s_2^1\right)^2}. \tag{2}$$

Also, particles consider nostalgia, w_n, and social influence, w_s, for deciding their directions. The weights, w_n and w_s, describe the importance of nostalgia and social influence for particles, where $w_n + w_s = 1$. We define the following expression for deciding the direction

$$\text{direction is towards} \begin{cases} \text{PB} & \text{if } (w_n d_{\text{LB}} - w_s d_{\text{GB}}) \leq 0, \\ \text{GB} & \text{if } (w_n d_{\text{LB}} - w_s d_{\text{GB}}) > 0, \end{cases} \tag{3}$$

```
(1)  Initialize and distribute particles
(2)  Loop while not (termination criteria (1) and (2))
(3)      For each particle:
(4)          If (PB > GB)
(5)              Replace GB and PB
(6)          Calculate PB
(7)          Decide the direction towards PB or GB
(8)          Move to new position
(9)      End of for
(10) End of loop
```

Algorithm 1: Generalized PSO algorithm.

where d_{LB} is the distance from the current location to the PB and d_{GB} is the distance from the current location to the GB. After calculating the direction, the particle moves toward the decided destination which is either PB or GB. During the optimization process, the GB is updated and broadcasted in the network when a solution with higher fitness value is found by a particle. After Γ iterations the particles gather (or converge) on the location with the highest fitness value and the algorithm terminates. This is referred to as termination criteria (1). The value of GB is considered as the solution of the optimization problem. Algorithm 1 shows the generalized PSO algorithm.

It should be noted that, as a result of heuristic nature of PSO, if the same GB value is found in more than one location the particles may not converge over a single solution space. To avoid probability of an infinite loop, in cases of equal GB values, and to allow management of the execution time, a maximum iteration number, $\Gamma_{\max}$, is set. When the process is stopped by reaching $\Gamma_{\max}$, called termination criteria (2), the GB with highest population of particles is chosen as the solution. Terminating the process in this way may lead to suboptimal results. Therefore, it is desired to increase the chance of reaching the optimal solution during a fixed period of time.

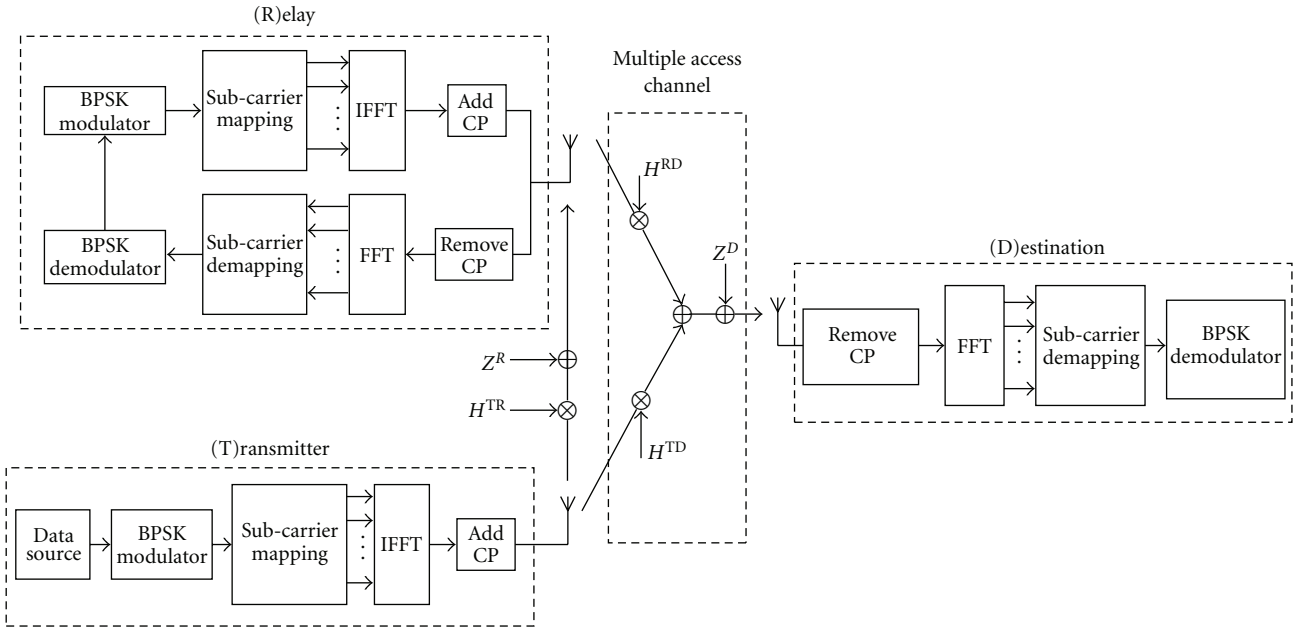

Figure 3: Block diagram of three cooperating nodes (transmitter-relay-destination) using orthogonal multicarrier modulation.

Increasing the number of particles, P, enables the algorithm to inspect the entire solution space before reaching $\Gamma_{\max}$. Both P and $\Gamma_{\max}$, are set during offline (by simulation) or online (after implementation) calibration process. The calibration process is performed in a solution space where the GB value is known. The process starts by setting P and $\Gamma_{\max}$ to a relatively large number in comparison to the number elements in solution space and then adjusting the parameters to reach a point where the algorithm converges over the GB in the given iteration time. The calibration process could be performed in intervals according to the dynamic nature of the solution space.

4. Adaptive MCCC Technique

Multicarrier communication is a well-known technique to achieve high performance in frequency selective channels [12]. It has been shown by adaptively allocating the subcarriers to the users with higher channel gains, the bit error rate performance of multicarrier communication is improved [13, 14]. However, the subcarriers with lower channel gains are discarded which results in reduction of spectral efficiency. To improve spectral efficiency, the MCCC technique has been proposed [10] that utilizes a higher number of subcarriers by means of cooperating with other nodes and utilizing them as a relay. In the following, the MCCC system model is described for three-node scenario to demonstrate benefit of employing PSO in adaptive resource allocation process. In the present study, only a single relay node is utilized to clearly illustrate the proposing idea of using PSO and the gain that can be achieved with low complexity. In principle the system could be extended to include more relays but at the cost of complexity. In the system model of adaptive MCCC, an ad hoc network which consists of autonomous nodes that are randomly distributed in a two-dimensional landscape is considered. It is assumed that all nodes are in radio coverage range of each other and support multiple connections. In the network layer, the nodes use the shortest path routing algorithm. At each instance, a transmitter node communicates to the destination using cooperative communication by transmitting the data through a relay node.

In the physical layer, the nodes use multicarrier modulation over N orthogonal subcarriers. The number of subcarriers used for the transmitter-relay (TR), transmitter-destination (TD), and relay-destination (RD) links are N^{TR}, N^{TD}, and N^{RD}, respectively, where $N^{TR} + N^{TD} \leq N$ and $N^{TR} = N^{RD}$. The subcarriers are exclusively allocated to each node.

The objective of cooperation is to maximize the bandwidth efficiency by utilizing the adaptively allocated subcarriers to the transmitter and relay nodes. The cooperation protocol consists of two time slots. In time slot one (TS1), the transmitter node allocates N^{TR} and N^{TD} subcarriers for TR and TD links and sends *different* data to the relay and destination nodes. In time slot two (TS2), the relay node allocates N^{RD} subcarriers to the RD link and sends the data received from the transmitter node in TS1 to the destination node where $N^{RD} = N^{TR}$. It is assumed that the nodes are fully synchronized and aware of the cooperative protocol. Next, we describe in more detail the MCCC transmission shown in Figure 3 employing the cooperation protocol in Table 1.

Time Slot 1. At the physical layer, the transmitter and relay nodes have binary modulated data $(-1, +1)$, using binary phase shift keying (BPSK), which are mapped to the allocated subcarriers. In the first time slot, the data symbols of the transmitter node are partitioned into two sections with

Table 1: Cooperation protocol.

	TS1 (Transmitter performs subcarrier allocation)	TS2 (Relay performs subcarrier allocation)
Transmitter	Tx(N^{TR}, N^{TD})	
Relay	Rx(N^{TR})	Tx(N^{RD})
Destination	Rx(N^{TD})	Rx(N^{RD})

lengths of N^{TR} and N^{TD}. The unallocated subcarriers do not carry any information data, but they are used in multicarrier modulation as null subcarriers. The partitioned symbols are then modulated over N orthogonal subcarriers using inverse fast Fourier transform (IFFT). It is assumed that the channel between each two nodes is a multipath fading channel with Rayleigh distribution and remains constant during each time slot of cooperation. Signal propagation in a multipath frequency selective channel causes intersymbol interference (ISI) at the receiver which severely increases the error rate. In multicarrier communication the transmitted symbol duration is increased and hence the effect of ISI is reduced [15]. To eliminate ISI from previous symbol, a CP with duration greater than the delay spread of the channel is added to the multicarrier symbol [12]. The transmitted and received symbols in TS1 over N subcarriers are given by

$$V^T = \sum_{u=0}^{N-1} k_u^T e^{j2\pi un/T_s}, \quad n = -L_{\mathrm{CP}}, \ldots, N-2, N-1,$$
$$R^R = V^T \cdot H^{\mathrm{TR}} + Z^R, \tag{4}$$
$$R^D = V^T \cdot H^{\mathrm{TD}} + Z^D,$$

where, k_u^T is the uth BPSK modulated symbol of the transmitter, T_S is the multicarrier symbol duration and L_{CP} is the length of CP. $H^{\mathrm{TR}} = [h_1^{\mathrm{TR}} e^{j\varnothing}, h_2^{\mathrm{TR}} e^{j\varnothing}, \ldots, h_N^{\mathrm{TR}} e^{j\varnothing}]$ and $H^{\mathrm{TD}} = [h_1^{\mathrm{TD}} e^{j\varnothing}, h_2^{\mathrm{TD}} e^{j\varnothing}, \ldots, h_N^{\mathrm{TD}} e^{j\varnothing}]$ are the vectors of complex fading coefficients for N subcarriers of the TR and TD links, respectively. Also, Z^R and Z^D are the additive white Gaussian noise at the receivers. In the relay and destination nodes, the CP is removed and the signal is passed through a fast Fourier transform (FFT). The received symbols are detected and demodulated by a BPSK demodulator [16].

Time Slot 2. In the second time slot, the relay node modulates the received data from the transmitter over N^{RD} subcarriers using a similar multicarrier modulation technique used in the transmitter. The received signal at the destination is demodulated as explained for the first time slot. The transmitted and received symbols in the second time slots are as follows:

$$V^R = \sum_{u=0}^{N-1} k_u^R e^{j2\pi un/T_s}, \quad n = -L_{\mathrm{CP}}, \ldots, N-2, N-1,$$
$$R^D = V^R . H^{RD} + Z^D, \tag{5}$$

where k_u^R is the uth BPSK modulated symbol of the relay node, $H^{\mathrm{RD}} = [h_1^{\mathrm{RD}} e^{j\varnothing}, h_2^{\mathrm{RD}} e^{j\varnothing}, \ldots, h_N^{\mathrm{RD}} e^{j\varnothing}]$ is the vector of complex fading coefficients for the N subcarriers of the RD link. It should be noted that with each transmission cycle, the transmitter divides a single set of data into two subsets, and the receiver collects all the transmitted data over two time slots. Therefore, the received data over two time slots, together, should be considered as the data received from the transmitter node. In the next section, PSO-aided adaptive resource allocation methods for the MCCC technique is proposed.

5. PSO-Aided Adaptive Resource Allocation in MCCC

The proposed generalized PSO model is applied to MCCC technique for adaptively performing subcarrier allocation and selecting a relay node. Figure 4, demonstrates how PSO is employed in MCCC in a seven-layer OSI network protocol stack where layer 1 and 3 are physical and network layers, respectively. Figure 4(a) illustrates the centralized PSO process using single layer and cross layer strategies for subcarrier allocation of MCCC protocol. In Figure 4(b), distributed PSO process in the network layer of all nodes is shown where the relay is selected from the autonomous nodes in the ad hoc network.

5.1. Centralized PSO for Subcarrier Allocation. PSO technique is a distributed algorithm by its nature. To extend the PSO to centralized optimizations, the particles need to be implemented as virtual particles (VPs). A VP is set of functions and memory spaces that, similar to a particle, is used to read the solution space, measure the fitness and store the PB. Each VP is also responsible to compare the PB value with the GB value in order to decide new direction and velocity. The VPs can be implemented as synchronized threads within a PSO software process. The PSO software process is responsible to share the GB among VPs and monitor the termination criteria. Using VPs enables the implementation of the proposed PSO on modern multithread digital signal processors (DSP) platforms [17]. In this section, PSO with VPs is applied to subcarrier allocation in the adaptive MCCC system. The objective is to minimize the transmit power by only using the subcarriers of good quality for that node. Two subcarrier allocation strategies are considered for the adaptive MCCC technique. For the first, resource allocation is based solely on the quality of the channel. In the second strategy a measure of distance between nodes and receiver is also considered.

5.1.1. Single Layer Strategy. Multipath channel results in having frequency selective fading over the subcarriers. Some subcarriers that are deeply faded in a link might have sufficient gain to be used for another link. Therefore, in subcarrier allocation strategy 1, adaptive allocation of frequencies based on channel gains is considered. In TS1, the subcarrier allocation for TD and TR links is performed at the transmitter node using centralized PSO where the subcarriers are exclusively allocated for each link. It is assumed that the transmitter node has knowledge of the TD and TR channels, and that the relay node has knowledge

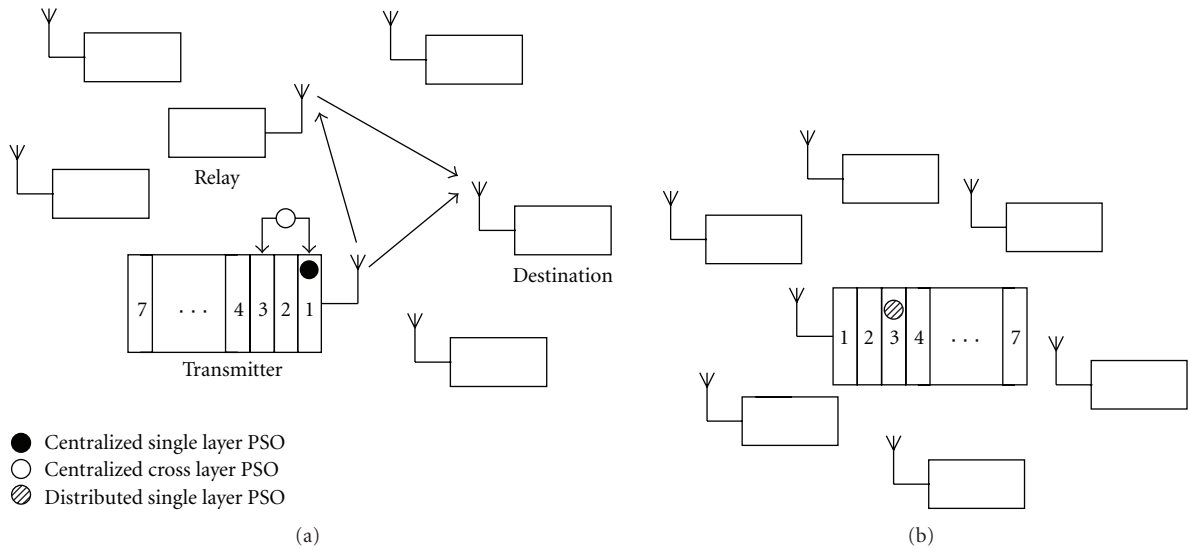

Figure 4: Utilization of generalized PSO in adaptive MCCC: (a) centralized single layer and cross layer PSO and (b) distributed single layer PSO.

of the RD channel. Allocation is performed by selecting the frequencies with the highest channel gain for each link, the gain information is obtained from the physical layer. The output results of the PSO algorithm are the sets of subcarriers with length of N^{TD} and N^{TR}. The subcarrier indexes are not necessary sequential. The proposed centralized PSO algorithm is used for selecting and allocating N subcarriers from the solution space. The solution space is the concatenation of the channel gains profiles for the TD and TR links described as

$$\begin{aligned} \mathrm{S} = &\left[\left|h_1^{\mathrm{TR}}e^{j\varnothing}\right|^2, \left|h_2^{\mathrm{TR}}e^{j\varnothing}\right|^2, \ldots, \left|h_N^{\mathrm{TR}}e^{j\varnothing}\right|^2\right] \\ &\odot \left[\left|h_1^{\mathrm{TD}}e^{j\varnothing}\right|^2, \left|h_2^{\mathrm{TD}}e^{j\varnothing}\right|^2, \ldots, \left|h_N^{\mathrm{TD}}e^{j\varnothing}\right|^2\right], \end{aligned} \tag{6}$$

where the [ ] ⊙ [ ] is the concatenation operator for two vectors. The length of the channel gains profile for two channels is $2N$. The fitness function, which is identical for nodes, is the nth subcarrier gain value, obtained from channel gains profile given by $f(n) = |h_n^{mm'}e^{j\varnothing}|^2$, where $|h_n^{mm'}e^{j\varnothing}|^2$ is the channel gain between the mth and the m'th node. The PSO algorithm terminates when one of the termination criteria (1) or (2) occurs. At this stage the solution with the GB value, which is the subcarrier with the highest channel gain for the node, is allocated to that node. The centralized PSO algorithm runs until N number of subcarriers is selected. While the PSO process is running, all VPs are flying over the solution space to find the subcarriers with the highest gain. For example, Figures 5(a) and 5(b) show snapshots of 30 VPs over a 128 subcarrier solution space before and after convergence which is the concatenation of two links (TD and TR) with 64 frequencies in each link. The PSO algorithm will choose the subcarriers with the highest gains.

In TS2, the subcarriers for the RD link are allocated from N frequencies. The allocation is performed by the relay node, and N^{RD} subcarriers with the highest channel gain in the RD link are chosen using similar method to that just described. However, the solution space will only contain the channel gains profile of the RD link described as following:

$$\mathrm{S} = \left[\left|h_1^{\mathrm{RD}}e^{j\varnothing}\right|^2, \left|h_2^{\mathrm{RD}}e^{j\varnothing}\right|^2, \ldots, \left|h_N^{\mathrm{RD}}e^{j\varnothing}\right|^2\right]. \tag{7}$$

The number of utilized subcarriers in TS2 is $N^{\mathrm{RD}} = N^{\mathrm{TR}}$, because the same amount of data received in TS1 over TR is transmitted to the destination using RD. Since the transmitter and the relay nodes communicate over two orthogonal time slots, having similar subcarriers used for the RD and TR links will not cause any interference.

5.1.2. Cross-Layer Strategy. In the second resource allocation strategy, a joint measure of channel gain and distance is considered to eliminate the effect of path loss by choosing more subcarriers from the links with a shorter distance. When employing strategy 1, a larger number of subcarriers are used for sending data of the transmitter compared to noncooperative adaptive multicarrier systems. The system can be further improved by considering the distance of the transmitter relay and transmitter destination. It is assumed that the relay node is physically located between the transmitter and destination nodes. The channel information is obtained from the physical layer whilst distance information is gathered from the network layer. In strategy 2 the effect of path loss is taken into account when selecting subcarriers. Assuming isotropic antenna on each node, the path-loss factor [18] for a signal is given by

$$C = \left(\frac{4\pi d}{\lambda}\right)^2, \tag{8}$$

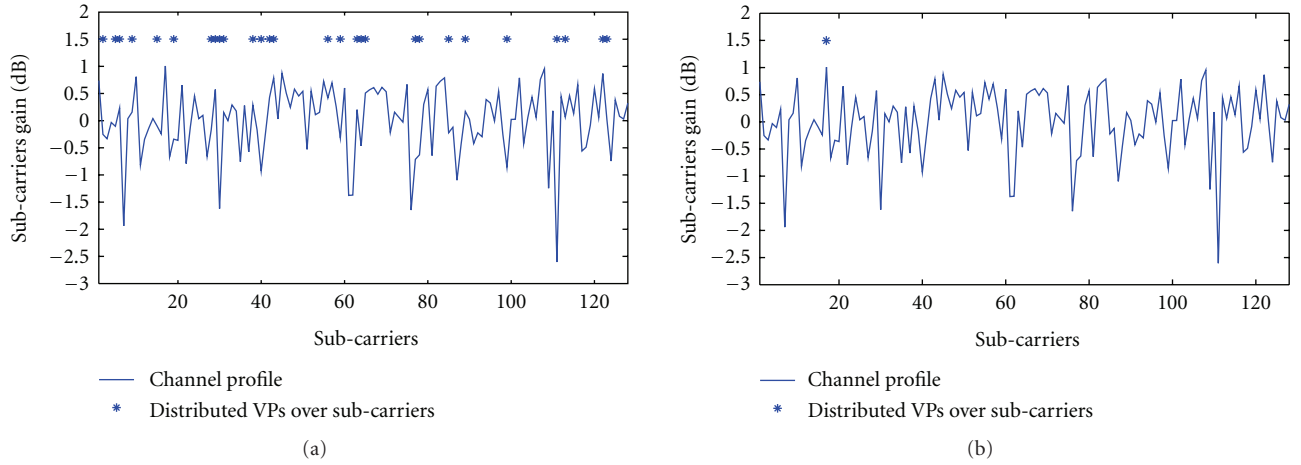

Figure 5: Snapshots of channel profile of TD and TR links and distributed VPs for a single user (a) before convergence and (b) after convergence.

where d is the distance between transmitter and receiver and λ is the wavelength of the signal. By normalizing the wavelength to unity, the cost of transmission over direct link, TD, and indirect link, TR, based on the path-loss is defined by

$$C_D = \sqrt{(x_T - x_D)^2 + (y_T - y_D)^2},$$
$$C_I = \sqrt{(x_T - x_R)^2 + (y_T - y_R)^2}, \tag{9}$$

where C_D is the cost of using direct link and C_I is the cost of using the indirect link. Further, (x_T,y_T), (x_D,y_D) and (x_R,y_R) are the coordinates of transmitter, destination, and relay nodes, respectively. In TS1, the channel gain per cost profile is considered as the solution space, S, and is formed by concatenating channel gains of TR and TD multiplied by the inverse of the cost as following:

$$S = (C_I)^{-1}\left[\left|h_1^{\mathrm{TR}}e^{j\varnothing}\right|^2, \left|h_2^{\mathrm{TR}}e^{j\varnothing}\right|^2, \ldots, \left|h_N^{\mathrm{TR}}e^{j\varnothing}\right|^2\right] \odot (C_D)^{-1}\left[\left|h_1^{\mathrm{TD}}e^{j\varnothing}\right|^2, \left|h_2^{\mathrm{TD}}e^{j\varnothing}\right|^2, \ldots, \left|h_N^{\mathrm{TD}}e^{j\varnothing}\right|^2\right]. \tag{10}$$

The N subcarriers with the highest fitness function are allocated from the TR and TD links. The fitness function is equal to the nth subcarrier channel gain per cost value. The centralized PSO algorithm, which runs at the transmitter node, terminates when one of the termination criteria (1) or (2) occurs. Figures 6(a) and 6(b) are the channel profiles of the TR and TD links when $N = 128$. As can be seen in Figure 6(c) after combining the channel profiles of two links and multiplying them by cost of each link, the fitness value of each subcarrier will indicate a joint measure of cost and channel gains. The subcarriers with lower cost stand higher than those with high cost. Figure 6(c) shows 30 randomly distributed VPs over the solution space before convergence. Based on centralized PSO with VPs, the subcarriers with the higher fitness values are selected. Figure 6(d) shows the VPs after convergence over the subcarrier with the highest fitness function. A threshold line is provided to demonstrate the difference between the channel gain per cost of subcarriers in direct and indirect links.

In TS2, a single link exists between relay and destination node and the distance only affects the scale of the solution space. Therefore, the subcarrier allocation is performed in a similar way to TS2 in strategy 1.

5.2. Distributed PSO for Relay Node Selection. As the subcarriers in adaptive MCCC system are exclusively allocated and the number of allocated subcarriers contributes to the data rate of the nodes, it is important to choose a node with low traffic for cooperation. Therefore, the node with the lowest traffic overhead in the network is chosen as the relay node. The selection process is performed once, prior to cooperation amongst nodes. Because of the distributed nature of the particles, the proposed distributed PSO model is suitable for efficient processing with different objectives. The two-dimensional solution space, S^1, S^2, is defined as following:

$$S^1 = \{s_1^1, s_2^1, \ldots, s_X^1\},$$
$$S^2 = \{s_1^2, s_2^2, \ldots, s_Y^2\}, \tag{11}$$

where X and Y are the dimensions of the landscape. The fitness function, $f(S^1, S^2)$, is equal to the inverse of the load of a node in location of (S^1, S^2). The load of a node is a measure of the tasks (i.e., packets) that need to be processed. It is assumed that this load remains constant during the optimization process. The processing load of a node in (x,y) with U number of task queues, is given by

$$f(S^1, S^2) = \frac{1}{\sum_{u=1}^{U} L_{s_x^1, s_y^2, u}}, \tag{12}$$

where $L_{s_x^1, s_y^2, u}$ is the size of the uth task queue. The distance is measured using (2) and the number of particles is less

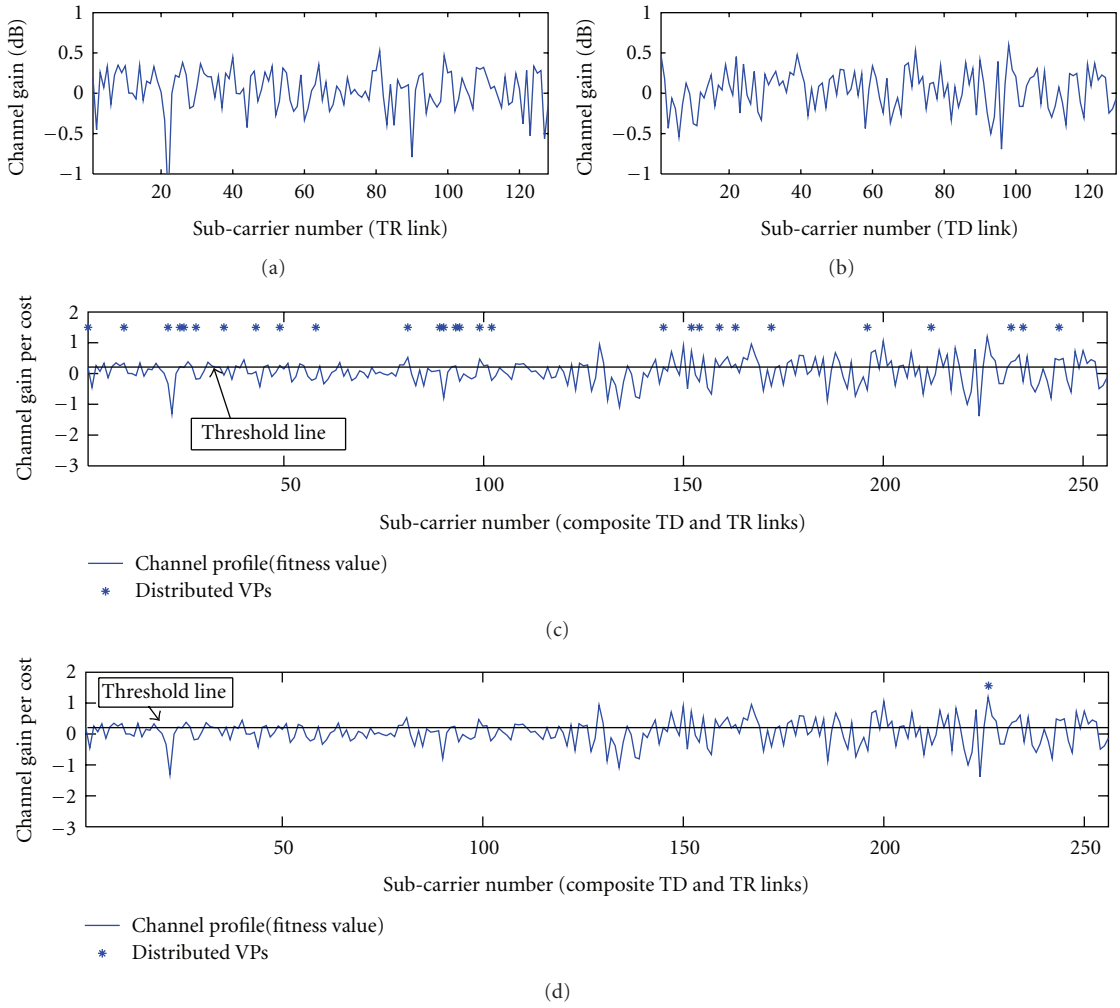

Figure 6: Snapshot of channel profile for $N = 128$ in the (a) TR link and (b) TD link and channel gain per cost profile (length of $2N$) with 30 randomly distributed VPs (c) before convergence and (d) after convergence.

than the number of nodes. The movement of particles in an ad hoc network introduces high traffic and computational complexity. Additionally, it may take a long time to converge. The traffic overhead is caused by the movement of particles and their associated information such as history of PB. To reduce the overheads, TPSO technique is proposed to adapt particles behaviour by changing w_n, w_s, and P values which affects social influence, nostalgia, and number of particles in the algorithm. The training process could be performed manually by observing the behaviour of the particles in a specific system or using artificial intelligence techniques such as neural networks [19].

At the beginning of the TPSO process, the particles are randomly distributed among the nodes. In the network, the packets move only through the single available route between two neighbouring nodes. Since the solution space is equal to the position of nodes, and is a sparse matrix, it is not expected to find any solution between two neighbouring nodes. Therefore, the movement of particles between two neighbouring nodes that is caused by uncertainty between nostalgia and social influence will not lead to finding a new PB or GB value. By manual training, the particles are forced to always follow the social influence (choosing the GB as the next destination) using the following configuration: $w_s = 1$, $w_n = 0$. This configuration will avoid redundant movements of the particles between two neighbouring nodes, thus reducing traffic and computational complexity.

Figure 7 shows the flowchart of the TPSO algorithm for an ad hoc network. The particles are implemented on each node using an identical software agent, called the particle process (PP). It is responsible to calculate, compare and update the PB and the GB values as well as moving the particle towards GB. Updating of GB is achieved using a broadcast algorithm in the network layer.

Since this updating is performed occasionally, the incurred overheads are neglected. The PP of a node runs only when at least one particle is over that node. Therefore, increasing the number of particles over a node will increase the computational complexity overhead. Particles move between two nodes by using a flag, carried by the data packets circulating in the network. The flag indicates when to run a PP process in a node and is also used for counting the PIDs

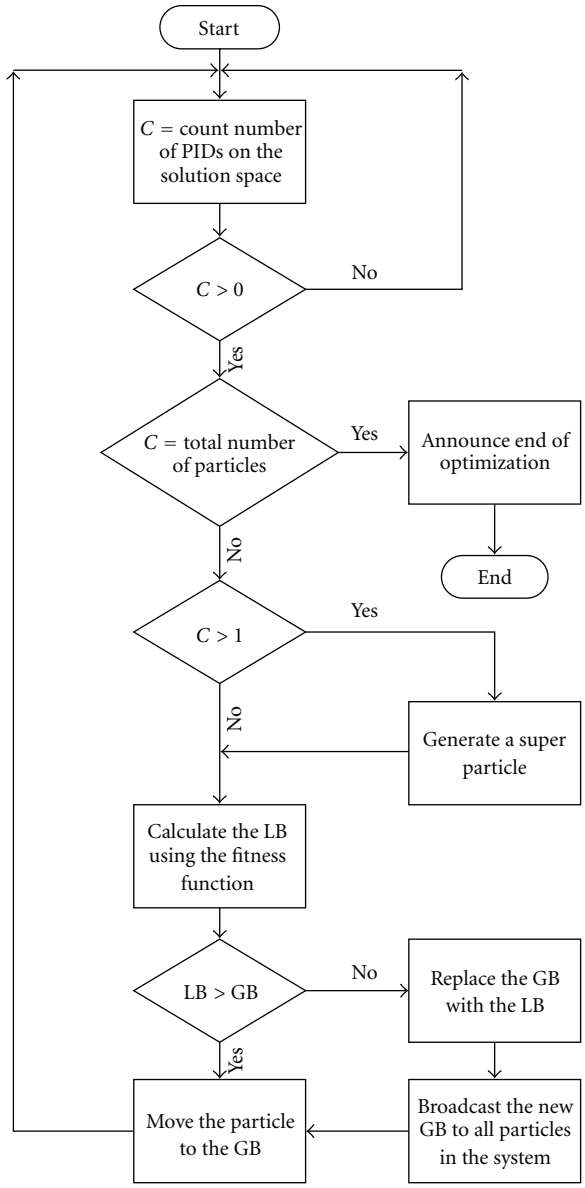

Figure 7: Flowchart of the TPSO algorithm for ad hoc network.

over a node. Since particles move among the nodes using data packets, their movement and direction depend on the availability of connection between the nodes.

In TPSO, all particles on a node have similar destinations which are either GB or the next hop towards GB. To further reduce the traffic overhead and computational complexity on a node, the particles are batched in a single super particle. The super particle which is the aggregation of all the particles on the node has a new PID that is known to the PP processes. The super particle calculates fitness and chooses the next direction in a similar method to normal particles. However, in order to check for termination criteria (1), mentioned in Section 3, the number of batched particles in a super particle is considered for calculating the number of PIDs in PP. For example, a node with 8 normal and a single super particle consisting of 10 particles, would have a total of 18 PIDs. Using super particles will gradually reduce the number of particles in running the system as the TPSO process continues as result of batching them. The TPSO terminates when one of the termination criteria, explained in Section 3, is met.

Figure 8 shows a snapshot of the proposed TPSO algorithm. The weights on each node represent the processing load on that node and the distributed circles on the nodes show the particles. As the process progresses, the particles converge over the node with the highest load. Based on the termination criteria explained before, the algorithm broadcasts the found solution to the other nodes when all particles have converged over a node or the maximum number of iterations has been reached.

6. Computation Complexity and Traffic Analysis

6.1. Computation Complexity. Computational complexity is a measure of how efficiently the available resources are utilized to perform the algorithm. One dimension of computational complexity is the time that the algorithm takes to terminate. Time complexity of an algorithm, regardless of execution platform specifications, is measured in terms of number of iterations using Big-O, $O(\cdot)$, notation [20] which, for the rest of paper, will be referred to as computational complexity.

Centralized PSO. The centralized PSO algorithm does not linearly search the solution space. Therefore, the possibility of finding the optimum solution before exploiting all possibilities is very high. Assuming that the order of an iterative optimization for N elements on average consists of two parts $O(\ ) \times O(G(\ ))$, where the first part corresponds to the number of iterations, and the second part is the complexity of the logic of the optimization algorithm. In multicarrier systems most of subcarrier allocation techniques use an unsorted list of subcarriers [21]. These techniques have high order of $O(N)$ [20], for the required linear search to find the highest gains for each user on each interval. The linear search process gets even more complex when the user needs an unknown number of subcarriers at each transmission. To reduce the required number of iterations the authors of [22] have used a sorted list of subcarriers. Using conventional sort algorithms, maintaining a sorted list of subcarriers in a time-variant channel introduces high order of $O(N \log N)$ [20]. PSO-aided subcarrier allocation uses an unsorted list of subcarriers to avoid the complexity overhead introduced by sorting. However, searches of the list are much simpler and faster than normal linear search algorithms. The complexity order of the PSO process based on the provided algorithm in Algorithm 1, using the principles of average case study [20], is given by $O(\log N)$. Using the $O(\cdot)$ function, Figure 9 shows the difference of linear search and sorted list selection algorithms in comparison to the PSO-aided technique for a different number of subcarriers. In addition, PSO is flexible on its parameters such as number of VPs and the employed fitness function, to enable controlling algorithm performance.

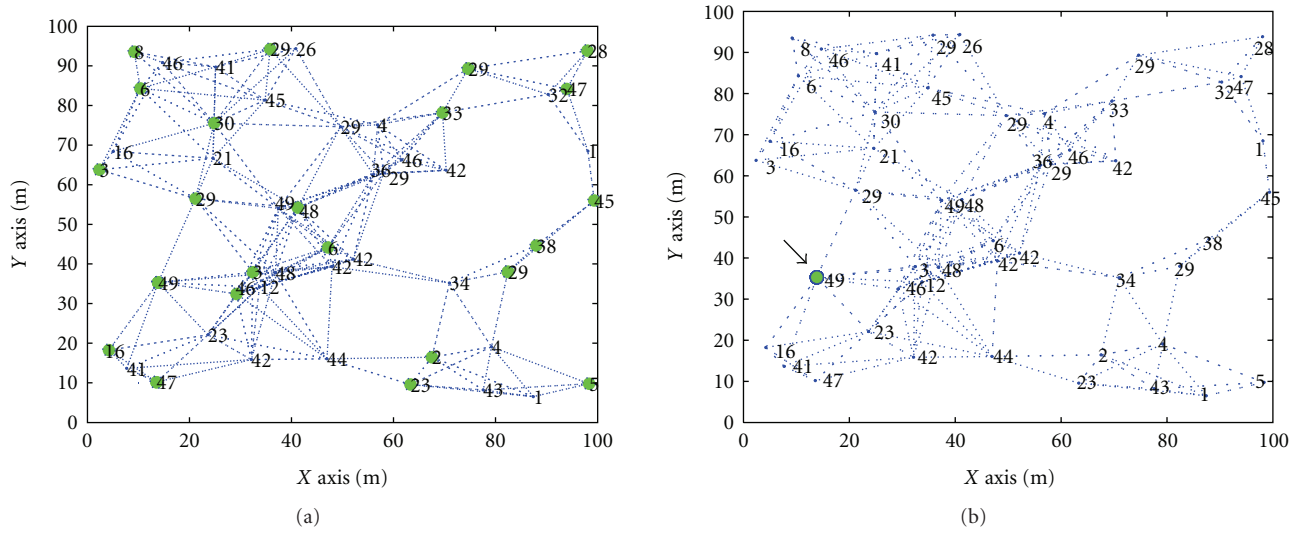

Figure 8: Snap shot of TPSO in ad hoc network with 50 nodes and 30 particles showing particles (a) before convergence, (b) after convergence.

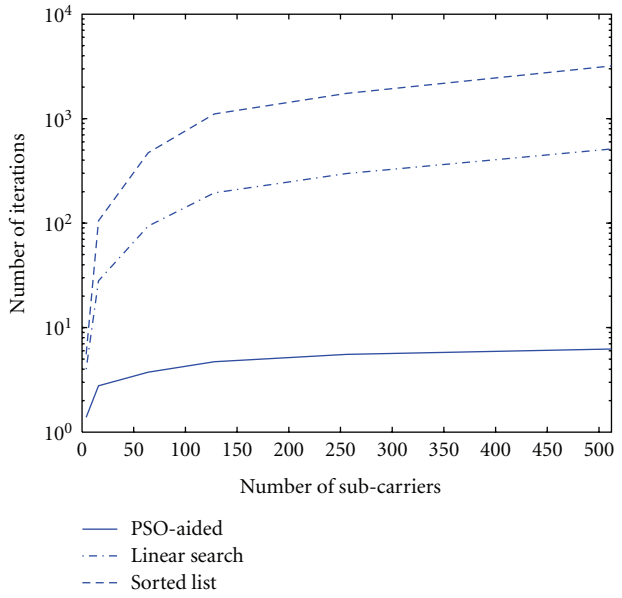

Figure 9: Complexity comparison of linear search, sorted list, and PSO-aided subcarrier allocation algorithms.

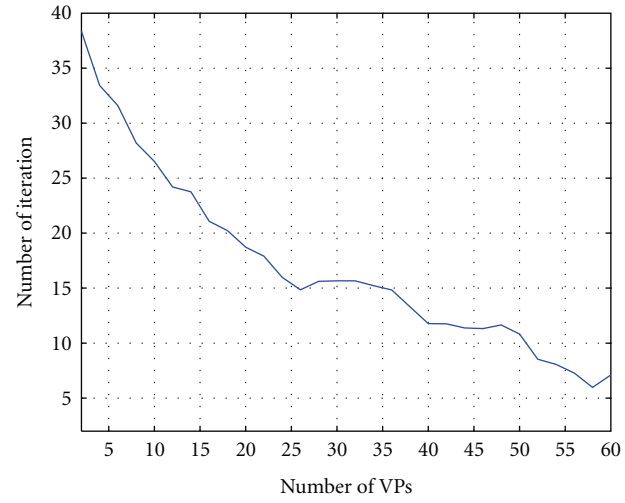

Figure 10: Iteration number for different number of VPs.

It is shown by simulation that increasing the number of VPs reduces the number of iterations needed to find the optimum result. Figure 10 shows number of iterations needed to find the GB value for a PSO-aided subcarrier allocation for 128 subcarriers in a node. As can be seen the number of iterations decreases as the number of VPs increases due to faster convergence. Although employing small number of VPs requires less memory, it may lead to a suboptimal result as not all the solution space may be explored.

Distributed PSO. In distributed scenarios the number of particles on a node impacts the number of iterations in the algorithm. Computational complexity of the distributed PSO on a single node is in order of $O(g(\Gamma))$ where $g(\Gamma)$ is the complexity function for Γ iterations on each node and is defined according to algorithm implementation. The complexity will increase to $O(Qg(\Gamma))$ when Q number of particles ($Q < P$) overlap on the node. In TPSO, when there is more than one particle over a node, they are collectively considered as one super particle. Each super particle is treated in a similar way to normal particles, and hence using super particles reduces the number of required packets. Since Q and Γ are reduced as a result of batching the particles with an identical destination to a super particle, the algorithm will run fewer iterations and hence the overall computational complexity will decrease.

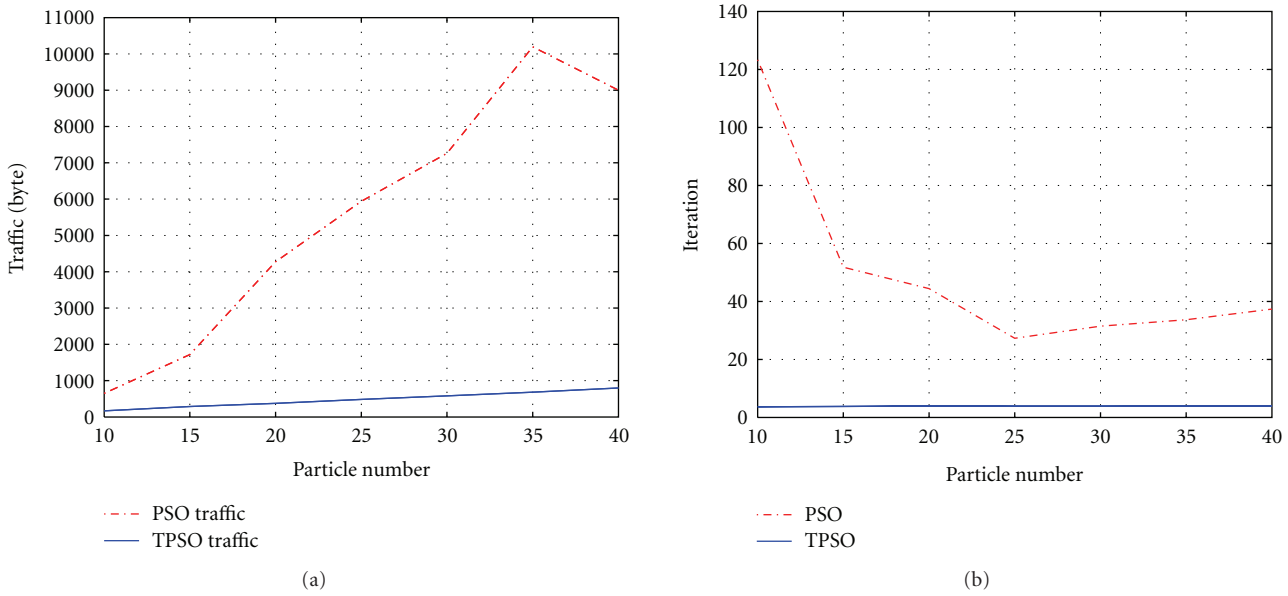

Figure 11: (a) TPSO traffic overhead in relation to PSO based on Table 2 and (b) convergence speed of particles (iterations) for TPSO and PSO algorithms in the ad hoc network with 50 nodes for different number of particles.

Table 2: PSO and TPSO packet sizes and description used in the simulation.

Packet type	Packet size in TPSO	Packet size in PSO	Description
GB_Broadcast	2	2	For broadcasting the value and location of the GB.
P_Move	1	4	For moving the particle from one node to another node. For PSO it contains PID, PB location and value and destination address. For the TPSO it only contains PID.
Terminate	1	1	A unique packet to indicate optimization termination

6.2. Traffic Analysis. In this section, traffic analysis for distributed PSO and TPSO are provided for a relay node selection process in an ad hoc network with 50 nodes. Both techniques are simulated and the gain of training the particles is demonstrated in relation to nontrained algorithm. In Table 2 we introduce the packets used in the simulated network. Assuming that each portion of data occupies only one byte, the size of packets for each packet type is calculated. In this experiment the overheads caused by the routing protocol of the network layer are not considered.

Figure 11(a) shows the average traffic overhead caused by P_Move packets for PSO and TPSO in the aforementioned

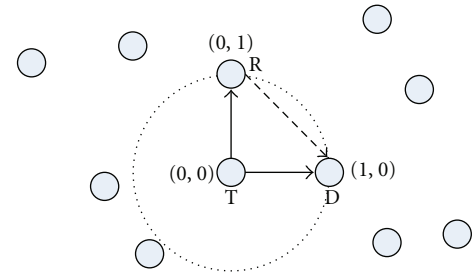

Figure 12: Three ad hoc nodes (transmitter, relay, and destination) using PSO-aided adaptive MCCC.

ad hoc network. The reduction in the traffic overhead is due to moving of less data between nodes. As a result of training, all particles always move towards the node with the GB value and do not return to their PB location. The GB location may change during the optimization process. However, at each interval all particles in the system move towards the same destination, the current GB. Since each super particle is treated in a similar way to normal particles, using super particles in TPSO reduces the number of required packets. In Figure 11(b) the average convergence time for PSO and TPSO based on the simulation results for different numbers of particles is demonstrated. The results show that when using TPSO the particles converge over the optimization solution with a near constant number of iteration in relation to PSO, where the achieved gain is due to training of particles. It should be noted that training the particles in this method is heavily dependent on the scenario which the PSO is trained for and hence it is not general.

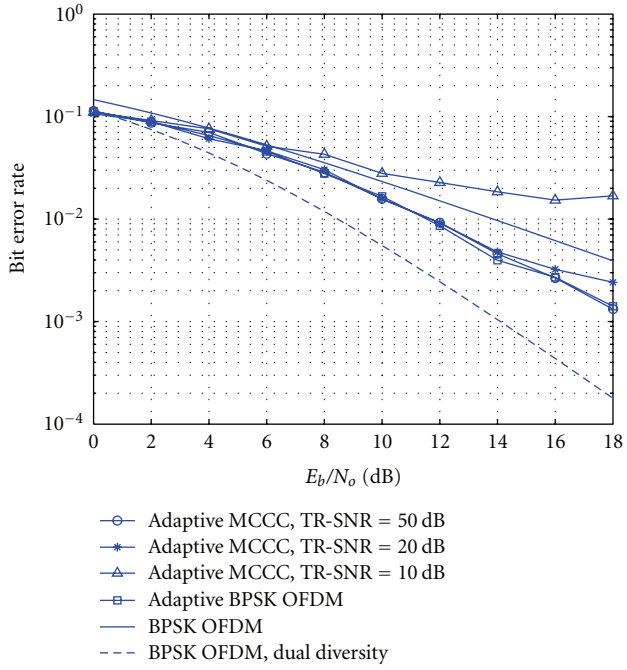

Figure 13: Bit error rate performance of adaptive MCCC technique using the first subcarrier allocation strategy for different TR-SNR.

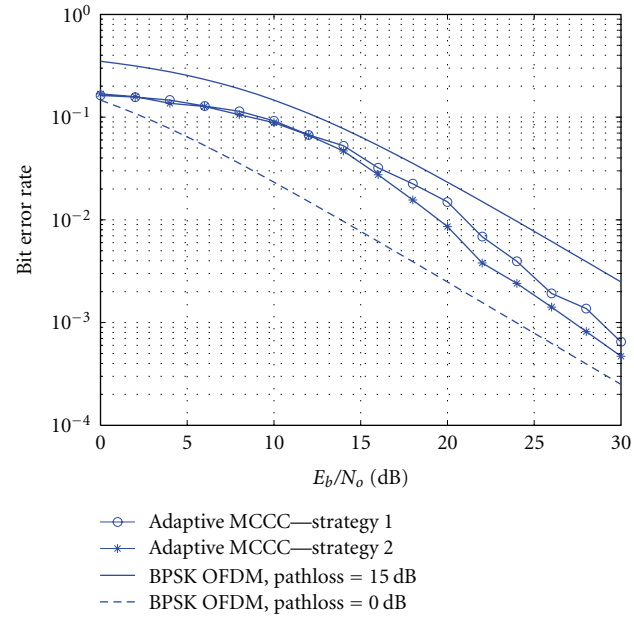

Figure 14: Bit error rate performance of adaptive MCCC technique of the first and second subcarrier allocation strategies where path-loss for TD and TR links is 15 dB and 20 dB, respectively.

7. Bit Error Rate Performance

In this section, the bit error rate performance of the PSO-aided adaptive MCCC technique is investigated by simulation. The bit error rate is a measure widely used to demonstrate and compare the performance of digital communication systems for a given signal to noise ratio (SNR) or energy per bit per noise (E_b/N_o) where the energy and noise are normalized to unity. In a binary modulated system, SNR and E_b/N_o are identical [18]. It is assumed that the relay node is selected by PSO in an ad hoc network. The nodes transmit using equal power and BPSK modulation over 128 subcarriers. The channel between each two nodes is assumed to be uncorrelated multipath fading with Rayleigh distribution where each subcarrier faces flat fading. Figure 12 shows the cooperative communicating nodes and their coordinates in the landscape. The results for the proposed resource allocation strategies are compared with single and dual receiver diversity BSPK OFDM using 128 subcarriers where all subcarriers, regardless of channel, are utilized for transmission [15]. It has been shown that the error rate performance of cooperative communications with high SNR channel between the cooperating nodes reaches the performance of dual receiver diversity [23]. Therefore, it is used as a bound for comparison purpose in cooperative systems. Utilizing diversity enables processing multireplica of a transmitted signal and hence significantly improves performance [18]. The performance of adaptive BPSK OFDM is also provided for comparison using the introduced adaptive OFDM with 30 VPs where half of the available subcarriers are adaptively allocated based on the channel gains [4].

Figure 13 shows the bit error rate performance of the PSO-aided adaptive MCCC system when $N/2$ of the available subcarriers using the first strategy. The results show that the performance of adaptive BPSK OFDM and adaptive MCCC are identical when the TR link has high SNR (i.e., 50 dB). High SNR in TR link reduces the error rate at the relay link and hence correctly received data bits are retransmitted by the relay node. It is shown that the TR-SNR affects the error rate performance at the destination. The bit error rate at the designation node increases when the quality of the TR links degrades (i.e., 10 and 20 dB). By choosing the relay node as the nearest node to the transmitter, the TR-SNR increases and the bit error rate reduces at the destination. Since the relay node does not repeat the data transmitted over the TD link, no diversity gain is expected. However, the error rate performance is improved in comparison to BPSK OFDM because of adaptive allocation of subcarriers. It should be noted, further performance improvements could be achieved by transmitting identical data over TD and TR links to gain from channel diversity.

In Figure 14, the bit error rate comparison between the two PSO-aided subcarrier allocation strategies is provided. In this simulation, the transmitted signal power is attenuated by the path loss over the TD and RD links. Having a normalized Gaussian noise, the effective SNR at the receiver is (E_b/N_o—path loss in dB). It is assumed that the path-loss of the TD link is 15 dB, and the path loss of the RD link is 20 dB. By calculating the effective SNR, the bit error rates in this figure are comparable to the results with the same E_b/N_o in Figure 13 (i.e., 20 dB in Figure 14 is equal to 5 dB in Figure 13). In the second resource allocation strategy, $C_D = 1$ and $C_I = \sqrt{2}$, using (9) and (12) based on the

coordinates given in Figure 12. As is shown in the figure, the adaptive MCCC technique using the second strategy has better performance in comparison to the first strategy. The reason is that the TR link has 5 dB higher path loss in comparison the TD link which is not considered in the first strategy.

8. Conclusion

In this paper, a generalized PSO model for adaptive resource allocation in communication networks has been proposed to reduce computational complexity in centralized and distributed resource allocation scenarios. The proposed model consists of PSO with VPs for centralized and TPSO for distributed optimizations which has been applied to resource allocation in the adaptive MCCC technique. Centralized PSO has been utilized for single layer and cross-layer subcarrier allocation to reduce computational complexity. Distributed TPSO has been utilized to reduce traffic overhead in adaptive relay node selection. The investigations show that the PSO technique provides less complex approach than linear and sorted list searches for subcarrier allocation which have been used in the literature. The introduced techniques are also flexible with regard to the number of particles and the fitness function. It has been shown that TPSO technique significantly reduces the traffic overhead of the node selection process in comparison to PSO. Moreover, the bit error rate performances for the single layer and cross layer strategies are demonstrated for the PSO-aided adaptive MCCC technique. Application of the proposed generalized PSO model to other communication techniques and scenarios are subject to further investigation.

References

[1] J. Kennedy and R. C. Eberhart, "Particle swarm optimization," in *Proceedings of the IEEE International Conference on Neural Networks IV*, vol. 4, pp. 1942–1948, December 1995.

[2] A. S. Tanenbaum, *Computer Networks*, Prentice Hall, New York, NY, USA, 4th edition, 2002.

[3] J. Robinson and Y. Rahmat-Samii, "Particle swarm optimization in electromagnetics," *IEEE Transactions on Antennas and Propagation*, vol. 52, no. 2, pp. 397–407, 2004.

[4] S. Ghcitanchi, F. H. Ali, and E. Stipidis, "Particle swarm optimization for resource allocation in OFDMA," in *Proceedings of the 15th International Conference on Digital Signal Processing (DSP '07)*, pp. 383–386, Cardiff, Wales, July 2007.

[5] S. Gheitanchi, F. H. Ali, and E. Stipidis, "Trained particle swarm optimization for collaborative computing networks," in *Proceedings of the Convention Communication, Interaction and Social Intelligence (AISB '08)*, vol. 11, pp. 7–12, Aberdeen, Scotland, 2008.

[6] J. Tillett, R. Rao, and F. Sahin, "Cluster-head identification in ad hoc sensor networks using particle swarm optimization," in *Proceedings of the IEEE Personal Wireless Communications*, pp. 201–205, 2002.

[7] S. M. Guru, S. K. Halgamuge, and S. Fernando, "Particle swarm optimisers for cluster formation in wireless sensor networks," in *Proceedings of the Intelligent Sensors, Sensor Networks and Information Processing Conference*, pp. 319–324, December 2005.

[8] X. Wu, L. Shu, J. Yang, H. Xu, J. Cho, and S. Lee, "Swarm based sensor deployment optimization in ad hoc sensor networks," in *Proceedings of the International Conference on Embedded Software and Systems (ICESS '05)*, vol. 3820 of *Lecture Notes in Computer Science*, pp. 533–541, 2005.

[9] P. Yuan, G.-X. Wang, and Y.-Y. Zhang, "Particle swarm optimization approach of solving communication optimization problems," *Journal of Northeastern University*, vol. 25, no. 10, pp. 934–937, 2004.

[10] S. Gheitanchi, F. H. Ali, and E. Stipidis, "Adaptive multi-carrier cooperative communication technique," in *Proceedings of the 5th International Conference on Broadband Communications, Networks, and Systems (BROADNETS '08)*, pp. 372–376, London, UK, September 2008.

[11] V. Srivastava and M. Motani, "Cross-layer design: a survey and the road ahead," *IEEE Communications Magazine*, vol. 43, no. 12, pp. 112–119, 2005.

[12] A. Goldsmith, *Wireless Communications*, Cambridge University Press, Cambridge, UK, 2005.

[13] A. Czylwik, "Adaptive OFDM for wideband radio channels," in *Proceedings of the IEEE Global Telecommunications Conference*, vol. 1, pp. 713–718, London, UK, 1996.

[14] C.-H. Yih and E. Geraniotis, "Adaptive modulation, power allocation and control for OFDM wireless networks," in *Proceedings of the 11th IEEE International Symposium on Personal, Indoor and Mobile Radio Communications (PIMRC '00)*, vol. 2, pp. 809–813, September 2000.

[15] L. Hanzo, M. Munster, B. J. Choi, and T. Keller, *OFDM and MC-CDMA for Broadband Multi-User Communications, WLANs and Broadcasting*, John Wiley & Sons, New York, NY, USA, 2003.

[16] B. Sklar, *Digital communications Fundamentals and Applications*, Prentice Hall, New York, NY, USA, 2001.

[17] Texas Instruments, 2009, www.TI.com.

[18] J. G. Proakis, *Digital Communications*, McGraw–Hill, New York, NY, USA, 4th edition, 2001.

[19] S. Haykin, *Neural Networks: A Comprehensive Foundation*, Pearson Education, Upper Saddle River, NJ, USA, 2nd edition, 1998.

[20] B. Raphael and I. Smith, *Fundamentals of Computer-Aided Engineering*, John Wiley & Sons, New York, NY, USA, 2003.

[21] H. Rohling, K. Brunighaus, and R. Grunheid, "Comparison of multiple access schemes for an OFDM downlink system," in *Multicarrier Spread Spectrum*, pp. 23–30, Kluwer Academic, Boston, Mass, USA, 1997.

[22] D. Kivanc, G. Li, and H. Liu, "Computationally efficient bandwidth allocation and power control for OFDMA," *IEEE Transactions on Wireless Communications*, vol. 2, no. 6, pp. 1150–1158, 2003.

[23] J. N. Laneman, D. N. C. Tse, and G. W. Wornell, "An efficient protocol for realizing cooperative diversity in wireless networks," in *Proceedings of the IEEE International Symposium on Information Theory (ISIT '01)*, p. 294, June 2001.